Thermal and Hydrodynamic Characteristics of Constructal Tree-Shaped Minichannel Heat Sink

Yongping Chen, Chengbin Zhang, Mingheng Shi, and Yingchun Yang
School of Energy and Environment, Southeast University, Nanjing, Jiangsu 210096, P.R. China

DOI 10.1002/aic.12135
Published online December 30, 2009 in Wiley InterScience (www.interscience.wiley.com).

A three-dimensional thermal and hydrodynamic model for constructal tree-shaped minichannel heat sink is developed. The heat and fluid flow in the constructal heat sink with an inlet hydraulic diameter of 4 mm are numerically analyzed, taking into consideration conjugate heat transfer in the channel walls. The pressure drop, temperature uniformity, and coefficient of performance (COP) of the constructal tree-shaped heat sink are evaluated and compared with those of the corresponding traditional serpentine flow pattern. The results indicate that the constructal tree-shaped minichannel heat sinks have considerable advantages over the traditional serpentine flow patterns in both heat transfer and pressure drop. The strong and weak heat flow can be effectively allocated in tree-shaped flow structures; hence, the inherent advantage of uniform temperature on the heating surface in the constructal tree-shaped heat sink is demonstrated. And in tree-shaped flow structures, the local pressure loss due to confluence flow is found to be larger than that due to diffluence flow. In addition, an aluminum constructal tree-shaped minichannel heat sink is fabricated to conduct the verification experiment. The experimentally measured temperature distribution and pressure drop are in agreement with the numerical simulation, which verifies that the present model is reasonable. © 2009 American Institute of Chemical Engineers *AIChE J,* 56: 2018–2029, 2010
Keywords: constructal, fluid flow, heat transfer, heat sink

Introduction

With the rapid growth in computational power of processor chips, thermal management has become a challenging factor, especially where strict limitation of space and operating costs are applied. Although heat sinks incorporating mini/microchannels have been found to be effective for these applications,[1,2] smaller sized channels can result in large pressure drops, and the temperature distributions are also dissatisfied, which may undermine the electronic performance. For this reason, it is desirable to design a flow heat transfer structure with better flow and thermal performance. Recent researches have demonstrated that the constructal theory[3,4] has been successfully used to optimize the flow configuration. Differing from the fractal geometry[5] which to describe natural phenomena by means of infinitely repetitive fracturing algorithms, the constructal theory is a completely deterministic theory of optimized and organized systems that evolve in time.

Inspiration for the optimization of many engineering problems can always be found in nature. For example, advanced heat and mass transfer efficiency can be found in mammalian circulatory and respiratory systems. The blood-circulating arteries and veins of human beings are self-organized as a branching vessel tree system. Predicting such geometric features is an essential objective of constructal theory

Correspondence concerning this article should be addressed to Y. Chen at ypchen@seu.edu.cn

which to describe the geometry and evolution of optimized and organized natural phenomena. Should we construct similar architectures to optimize the heat and mass transfer system, more advanced transport performance may be acquired. The important applications of the tree-shaped architectures of constructal theory have been found in electronics cooling,[6] fuel cells,[7–11] traffic,[12] etc. More specifically, the constructal tree-shaped mini/microchannel heat sink has been developed in the context of optimization design of cooling system for electronic chips.

Bejan[6] first proposed trees in electronics cooling with high conductivity path when he stated the constructal law. It is shown that, the tree-like network can be determined theoretically in a definite time direction, from the smallest building block (elemental system) to larger building blocks (assemblies). And then Bejan and Errera[13] outlined a strategy for constructing the architecture of the volume-to-point path such that the fluid flow resistance is minimal, i.e., deterministic tree networks for fluid flow was introduced, which extended the constructal method from heat conduction[6] to fluid flow. Later, Bejan[14] showed that the total heat current convected by a double tree is proportional to the total volume raised to a power of three-fourth, and presented a constructal principle in nature and engineering.[15,16]

As declared by Kearney,[17] the equipment built with self-similar characteristics offer advantages over traditional fluid mixers and distributors. Luo et al.[18] examined experimentally the effects of constructal distributors or collectors, built on a binary pattern of pores, on flow equidistribution in a multi-channel heat exchanger. Pence[19,20] and Alharbi et al.[21,22] proposed a tree-shaped microchannel network for the convective cooling of microelectronic components with disk geometric shapes. In particular, Daniels et al.[23,24] extended the application of tree-shaped net from single phase flow to two-phase flow, the adiabatic flow boiling in such tree-shaped microchannel network was investigated. Wechsatol et al.[25] and Ghodoossi[26,27] also optimized tree-shaped networks for fluid flow in the disk-shaped body. In the real application, the square or rectangular shaped heat sink is preferred due to the fact that the majority of the electronic or electrical components are square or rectangular rather than disk shape. However, the free circulation of the cooling fluid is difficult to be realized in a single layer tree-like network with a rectangular shape. To solve this problem, Chen and Cheng[28] designed a new sandwich structure tree-like channel net heat sink for cooling of rectangular chips. A comparison between the new design and the traditional parallel net showed that the new tree-like microchannel net has a stronger heat transfer capability and requires lower pumping power.

Senn and Poulikakos[7] numerically investigated the laminar convective heat transfer and pressure drop characteristics in tree-like microchannel nets[28] and proposed their application for thermal management in polymer electrolyte fuel cells. It was found that the tree-like nets own the intrinsic advantage with respect to both heat transfer and pressure drop, and the secondary flow motions initiated at bifurcations can effectively enhance thermal mixing and hence, heat transfer. Recognizing the significant potential of tree branching concepts in thermal management, Senn and Poulikakos[8,9] then introduced the constructal tree-like channel networks as a fuel cell fluid distribution concept to optimize the structure of polymer electrolyte fuel cells, and designed pyramidal direct methanol fuel cells based on the tree network distribution channels. Xu and Yu[29] analyzed the transport properties including electrical conductivity, heat conduction, convective heat transfer, laminar flow, and turbulent flow in the tree-like networks and derived the scaling exponents of the transport properties in the networks. Wang et al.[30,31] investigated the fluid flow and heat transfer characteristics of tree-shaped microchannel nets having disk and rectangular shapes, respectively. The simulation results indicated that the tree-shaped microchannel networks have certain advantages over conventional parallel channel nets including more uniform temperature distribution and better stability in case of accidental blockage in channel segments. Hong et al.[32,33] studied the characteristics of a modified tree-shaped microchannel network heat sink by solving 3D N-S equations and energy conservation equations. Comparisons between the modified tree-shaped network and the traditional parallel network indicated that the modified tree-shaped microchannel network has lower pressure drop, smaller thermal resistance and better temperature uniformity. However, it must be pointed out that despite the fact that the whole tree-shaped system can offer certain advantages of temperature distribution and pumping power requests, the junction losses, which are generated by the bifurcation, can not be neglected and must be taken into account in the optimization.[34] Wang et al.[35] simulated the effect of the bifurcation angles in the constructal nets on the fluid flow and heat transfer characteristics, and they showed that the bifurcation angle was an important factor for the performance of tree-like cooling nets.

Despite there has been a great deal of interest in tree-shaped networks,[6–39] their implementation has been limited by the complicated structure of tree-shaped nets and the large computing requirements; a majority of the available numerical analyses are based on one- or two-dimensional models. Although Senn and Poulikakos[7] developed a three-dimensional model and obtained a very useful finding of the convective heat transfer enhancement by the bifurcation, the conjugate heat transfer in channel walls was not taken into consideration in the model and the temperature distribution of heating surface was not proposed, which is important to evaluate the temperature uniformity. And only a single layer tree-like net was considered in the three-dimensional simulation by Hong et al.[32,33] The understanding of the heat and mass transfer mechanisms in tree-shaped heat sinks, especially the influence of the diffluence and confluence on the flow and heat characteristics, is still insufficient for the current situation. In addition, the temperature distribution at the heating surface, which can intuitively present the superior temperature uniformity of the tree-shaped channel heat sink, has not been studied enough. The temperature distribution of heating surface could be demonstrated so as to evaluate the temperature uniformity only if the coupling between heat conduction in the solid and heat convection in the fluid is considered. More importantly, the available simulation results are still lack of experimental verification.

Therefore, this article develops and numerically analyzes a three-dimensional model for heat and flow in sandwich structure constructal tree-shaped minichannel heat sinks, taking into consideration the conjugate heat transfer in channel

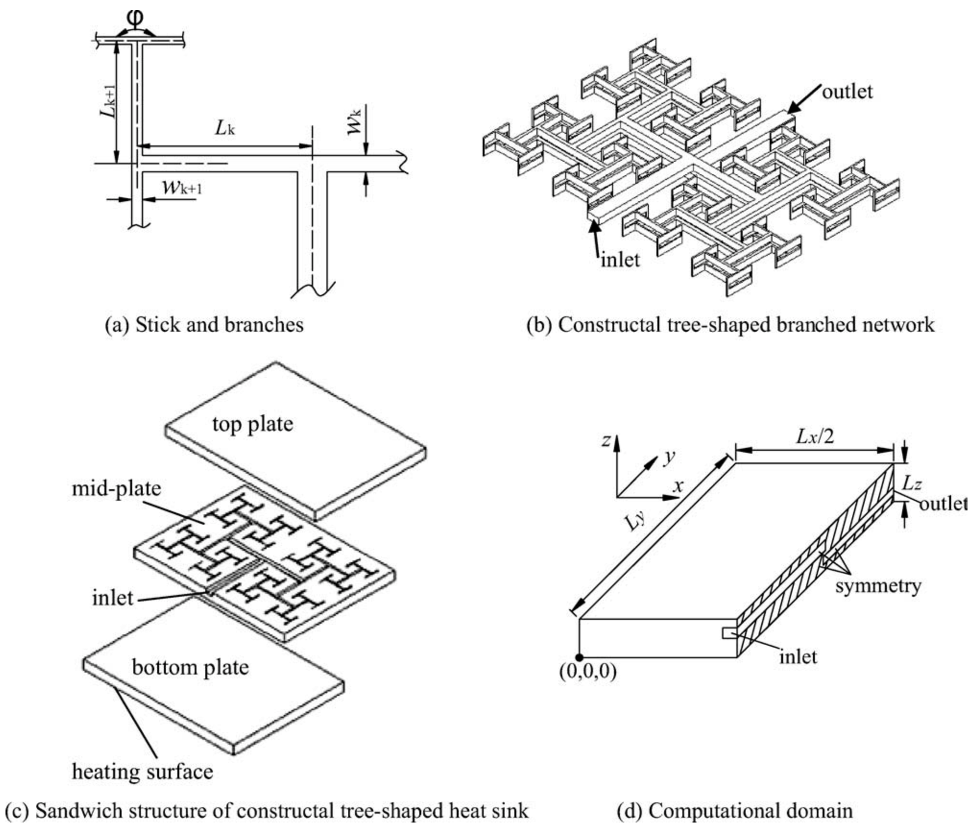

Figure 1. Schematic of constructal tree-shaped minichannel heat sink.

walls. The uniform temperature distribution on heating surface are identified and discussed. And the coefficient of performance of the constructal tree-shaped heat sink is evaluated. Furthermore, a constructal tree-shaped minichannel heat sink is designed and fabricated on aluminum substrate, and the experiment is conducted to verify the numerical simulation and examine the advantages of superior temperature uniformity and pumping power requests.

Constructal Tree-Shaped Net of Rectangular Shape

As proposed by Chen and Cheng,[28] a tree-shaped channel net with rectangular shape shown in Figure 1 can be constructed as:

a. Suppose that every channel is divided into two branches at the next level as shown in Figure 1a, i.e., a single channel bifurcates and $N = 2$, the branching angle φ is 180°, and the tree-shaped net has six branching levels.

b. We define that the ratio of the length of the channel at the $(k + 1)$th branching level to the length of the channel at the kth branching level as

$$\frac{L_{k+1}}{L_k} = N^{-1/D} \tag{1}$$

It follows that

$$L_k = L_0 N^{-k/D} \tag{2}$$

where L_0 is the length at the 0th branching level. As suggested by Chen and Cheng,[28] the thermal efficiency at the dimension $D = 2$ will be the highest, so $D = 2$ is chosen in this paper.

c. If the branch hydraulic diameters before and after bifurcation are denoted by d_k and d_{k+1}, respectively, the hydraulic diameter ratio is defined as

$$\frac{d_{k+1}}{d_k} = N^{-1/\Delta} \tag{3}$$

where Δ is the diameter dimension. Murray[40] studied the blood flow in vascular system and found the optimal diameter dimension is 3. Mandelbrot[5] pointed out that the diameter dimension of human lung vessel tree is 3. Bejan et al.[39] also proposed an optimal constructal tree diameter ratio of $2^{1/3}$ for laminar flow. Therefore, $\Delta = 3$ is chosen. It follows that

$$d_k = d_0 N^{-k/\Delta} \tag{4}$$

where d_0 is the initial hydraulic diameter of channel net.

As shown in Figure 1b, to have free circulation of the coolant and a uniform heat transfer, the heat sink is designed to have a top and a bottom circulation pattern in the middle plate. The bottom circulation pattern has the same distribution of the channel net as the top one except that the inlet channel on the top and the outlet channel on the bottom pointed towards opposite direction. The channel of the highest branching level ($k = 6$) on the top communicates with the channel of the highest branching level on the bottom.

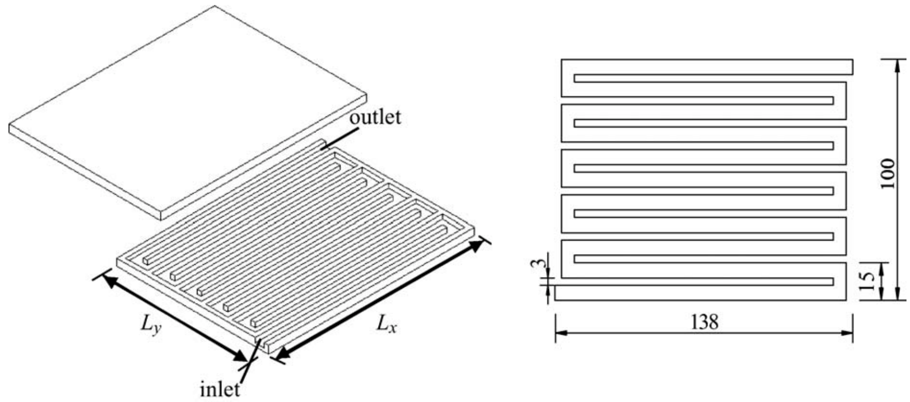

(a) Serpentine flow pattern heat sink (b) Serpentine flow pattern (unit : mm)

Figure 2. Schematic of serpentine flow pattern heat sink.

The cross section of each branching level channel is rectangular and has the same height of h. The schematic of constructal tree-shaped minichannel heat sink with the width $L_y = 100$ mm, length $L_x = 138$ mm and thickness $L_z = 16$ mm, which is composed of three aluminum plates, is shown in Figure 1c. Considering that the heat sink is symmetric to the plane at $x = L_x/2$, half of the whole heat sink, shown in Figure 1d, is selected as the computational domain to simplify the calculation.

To compare the thermal performance of constructal heat sink, a serpentine flow pattern heat sink as shown in Figure 2 with the same heating surface dimension is designed. The serpentine channel has the same cross section with the initial channel in constructal net. The heat transfer area of the serpentine channel is also equal to that in constructal net. Table 1 presents the geometry parameters for constructal and serpentine channel heat sink.

Mathematical Model

For the computational domain as shown in Figure 1d, adiabatic boundary conditions are applied to the boundaries of the solid region except the bottom surface. Uniform heat flux $q = 2.5$ W/cm^2 or constant wall temperature $T_b = 60°$C are imposed at the bottom surface, while a symmetric boundary condition is applied to the section at $x = L_x/2$. DI water at 20°C is used as the coolant. The velocity of the fluid entering the inlet of the heat sink is specified. To simplify the model of fluid flow and heat transfer, the following assumptions are applied:

(1) Laminar flow;
(2) steady fluid flow and heat transfer;
(3) constant solid and fluid properties;
(4) negligible gravity.

Governing equations

For the fluid,
Continuity

$$\nabla \cdot \vec{V} = 0 \tag{5}$$

Momentum

$$\rho_f(\vec{V} \cdot \nabla\vec{V}) = -\nabla P + \mu_f \nabla^2 \vec{V} \tag{6}$$

Energy

$$\rho_f c_{p,f}(\vec{V} \cdot \nabla T) = \lambda_f \nabla^2 T \tag{7}$$

For the solid, the energy equation is

$$\lambda_s \nabla^2 T = 0 \tag{8}$$

Table 1. Geometry Parameters for Constructal and Serpentine Channel Heat Sink

Surface Area		13,800 mm^2		Convective Area			19,816.9 mm^2		
Dimensions of heat sink		$L_x = 138$ mm $L_y = 100$ mm $L_z = 16$ mm		Inlet/outlet channel dimensions			$w = 6$ mm; $h = 3$ mm		
Channel dimensions	Tree shaped	k	0	1	2	3	4	5	6
		L_k/mm	50.00	35.35	25.00	17.68	12.50	8.84	6.25
		d_k/mm	4.00	3.18	2.52	2.00	1.59	1.26	1.00
		h_k/mm	3	3	3	3	3	3	3
		w_k/mm	6.00	3.37	2.17	1.50	1.08	0.80	0.60
		Total length	311.24 mm						
	Serpentine	Cross section	$w = 6$mm; $h = 3$mm						
		Total length	1202.5 mm						

w is the width, h is the height.

Boundary conditions

The non-slip boundary condition is applied on wall

$$u_\Gamma = v_\Gamma = w_\Gamma = 0 \tag{9}$$

A uniform velocity is applied at the channel inlet

$$y = 0, \quad u = 0, \; v = \frac{\mu Re_{k=0}}{\rho_f d_0}, \; w = 0 \tag{10}$$

The flow is fully developed at the channel outlet

$$y = L_y, \qquad \frac{\partial u}{\partial y} = 0, \; \frac{\partial v}{\partial y} = 0, \; \frac{\partial w}{\partial y} = 0 \tag{11}$$

Adiabatic boundary conditions

$$x = 0, \qquad -\lambda_s \frac{\partial T_s}{\partial x} = 0 \tag{12a}$$

$$y = 0 \; or \; y = L_y, \qquad -\lambda_s \frac{\partial T_s}{\partial y} = 0 \tag{12b}$$

$$z = L_z, \qquad -\lambda_s \frac{\partial T_s}{\partial z} = 0 \tag{12c}$$

Heating surface conditions

a. Constant heat flux at the bottom surface

$$z = 0, \qquad -\lambda_s \frac{\partial T_s}{\partial z} = q \tag{13a}$$

or

b. Constant wall temperature at the bottom surface

$$z = 0, \qquad T = T_b \tag{13b}$$

The fluid temperature at the inlet is given as

$$y = 0, \qquad T_f = T_{in} \tag{14}$$

At the channel outlet the flow is assumed to be thermally fully developed

$$y = L_y, \qquad \frac{\partial T_f}{\partial y} = 0 \tag{15}$$

Heat transfer in the heat sink is a conjugate problem which combines heat conduction in the solid and convective heat transfer to the cooling fluid. The two heat transfer modes are coupled by the continuities of temperature and heat flux at the interface between the solid and fluid, which are expressed as

$$T_{s,\Gamma} = T_{f,\Gamma} \tag{16}$$

$$-\lambda_s \left(\frac{\partial T_s}{\partial n} \bigg|_\Gamma \right) = -\lambda_f \left(\frac{\partial T_f}{\partial n} \bigg|_\Gamma \right) \tag{17}$$

Numerical solution

The numerical solution of the governing differential Eqs. 5–8 for the constructal tree-shaped channel heat sink is obtained by means of the control volume finite-difference technique and the SIMPLE algorithm. For the complex geometry structure involved (see Figure 1c), a hybrid hexahedron/prism mesh is applied to arrive at a solution. A non-uniform grid arrangement with a large number of grid points in bifurcations and near the channel wall is used to consider the effect of the bifurcation and boundary layer flow. The resulting system of algebraic equations is solved using the Gauss-Seidal iterative technique, with successive over-relaxation to improve the convergence time.

The numerical code is verified in a number of ways to ensure the validity of the numerical analysis. A grid independence test is conducted using several different mesh sizes. This test proved that the results based on the final grid system presented in this paper are independent of the mesh size. In addition, the solution is regarded as convergent, not only by examining residual levels of velocity below 10^{-6}, but also by monitoring relevant integrated quantities and checking for heat and mass balances.

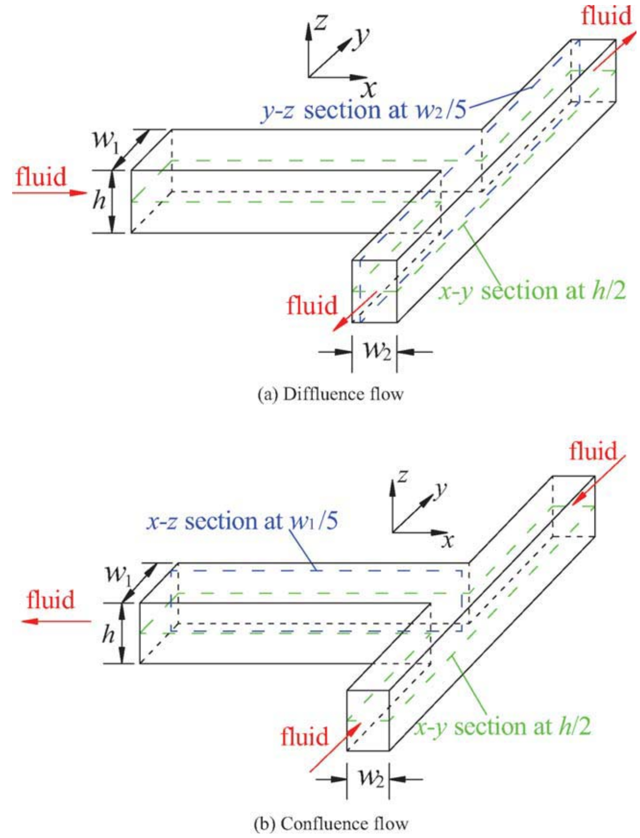

Figure 3. Schematic of velocity sections for fluid flow.

[Color figure can be viewed in the online issue, which is available at www.interscience.wiley.com.]

Numerical Results and Discussion

Hydrodynamic characteristics

In the tree net, both the diffluence flow (from kth to (k + 1)th branching level) in the top network and confluence flow (from (k + 1)th to kth branching level) in the bottom network over bifurcations as shown in Figure 3 induces swirl patterns, i.e. the secondary flow is generated near the

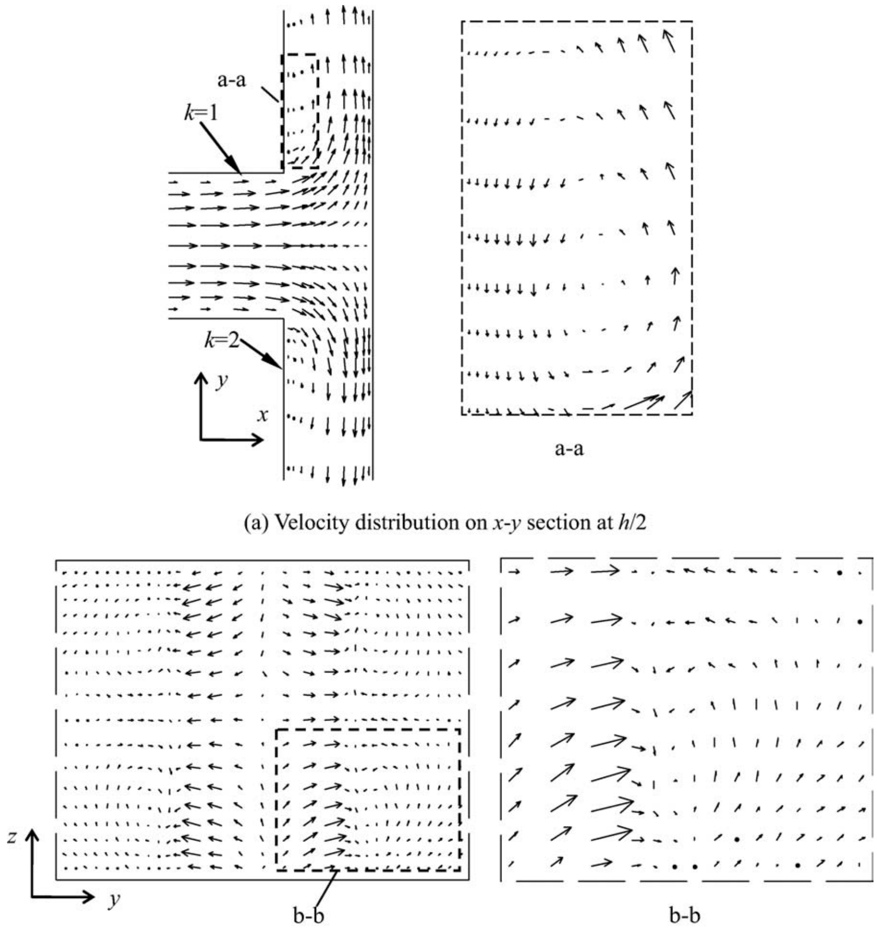

Figure 4. Velocity distribution at the bifurcation for diffluence flow.

bifurcations. To present a clear explanation for the effect of bifurcation on fluid flow, the velocity vectors at typical branches including both diffluence and confluence flow (inlet Reynolds number is 1500) are presented in Figures 4 and 5 with the corresponding velocity sections shown in Figure 3. As reported earlier by Senn and Poulikakos,[7] due to the presence of secondary flow, the fluid at the center of the channel is delivered toward the channel wall and then mixes with the fluid close to the channel wall. This fluid flow behavior can effectively enhance laminar mixing and heat transfer.

Fluid flow in constructal tree-shaped channel is not only beneficial to enhance heat transfer, but also reduces pumping power when compared with the serpentine flow pattern. As shown in Figure 6, in spite of the large number of bifurcations in the tree net compared to a much lower number of turns in the serpentine flow pattern, the constructal tree-shaped channel proves significantly beneficial in terms of pressure drop.

It is important to note that, in the constructal tree-shaped channel network, the fluid flow behavior in the top and bottom channels for the same branching level are different, especially at bifurcations where diffluence or confluence flow occurs (see Figures 4 and 5). Figure 7 compares the pressure drop across each branching level for top and bottom channels with the inlet Reynolds number of 1500. As shown in the figure, the pressure drop for each branching level in the bottom channels where the confluence flow occurs is larger than that in the top channels where the diffluence flow occurs. This phenomenon implies that the local pressure loss due to confluence flow is larger than that due to diffluence flow, and also verifies that the effects of bifurcation on pressure drop for the top and bottom channels are different.

Temperature distribution

Temperature distribution is one of the key factors in the thermal performance for heat sinks. With consideration of conjugate heat transfer in the channel walls, a more realistic characterization of convection heat transfer in constructal tree-shaped channel heat sink can be specified, and hence, the temperature distributions of heat sink can be intuitively presented. Figure 8 compares the temperature distributions on several typical sections of the constructal tree-shaped minichannel heat sink under constant heat flux and the corresponding serpentine flow pattern heat sink with the same inlet geometry, heat transfer area and heating surface dimension. As shown in Figures 8a,b, the temperature distributions on the heating surface of two heat sinks are evidently different, and the inherent advantage of uniform temperature in constructal heat sink is demonstrated. As the channel layout

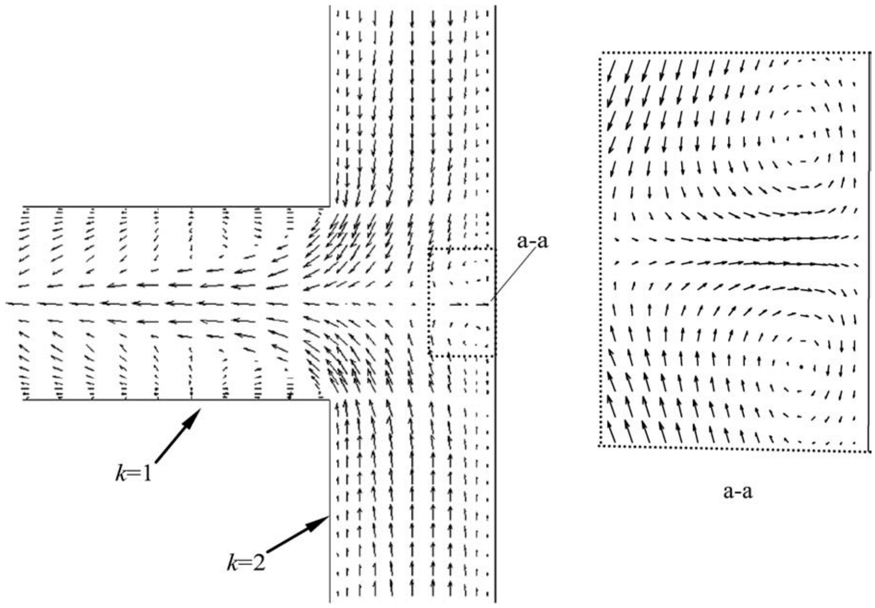

(a) Velocity distribution on x-y section at $h/2$

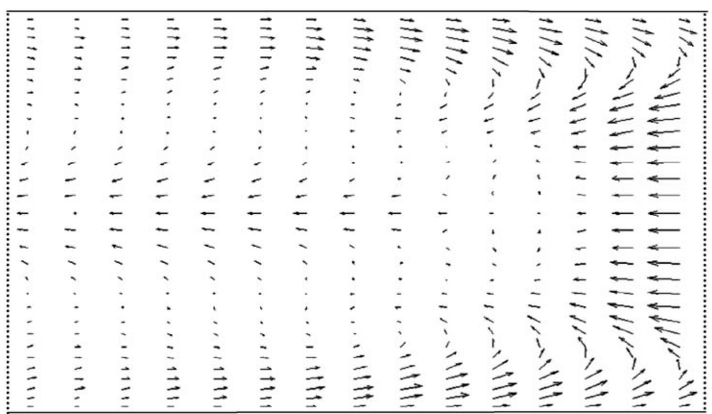

(b) Velocity distribution on x-z section at $w_1/5$

Figure 5. Velocity distribution at the bifurcation for confluence flow.

is in a fashion of net, the distribution of strong and weak heat flow can be effectively allocated. The heat transfer is interacted among different branching level channels in the constructal tree-shaped minichannel heat sink, and it is difficult to develop the local hot spots. The temperature increases gradually from the centre to the periphery of the heating surface in the constructal heat sink, but the increasing magnitude of temperature is small. With the inlet Reynolds number of 1500, the maximum temperature difference on the heating surface is 3.36°C. However, the interactions of the heat transfer among the channels in the serpentine flow pattern heat sink are much weaker, and a larger temperature difference, 9.87°C, occurs between the inlet side and the outlet.

Figures 8c and d show the temperature distributions on the x-y sections at $h/2$ of the top and bottom constructal tree-shaped minichannel networks respectively. As shown in Figure 8c, the increase of fluid temperature in the 0, 1, and 2 branching levels of the top constructal tree-shaped minichannel network is very small. However, the fluid temperature raise significantly when passing through the latter four branching level channels, which have a smaller flow rate and larger heat transfer area per unit volume, and this result

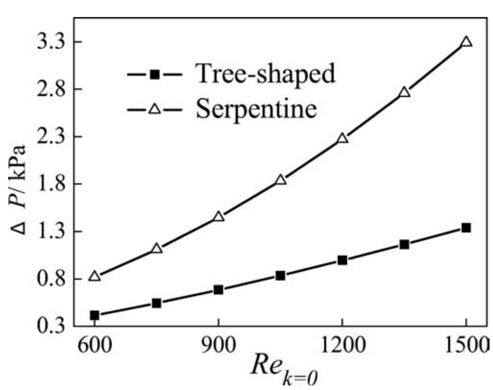

Figure 6. Pressure drop vs. inlet Reynolds number.

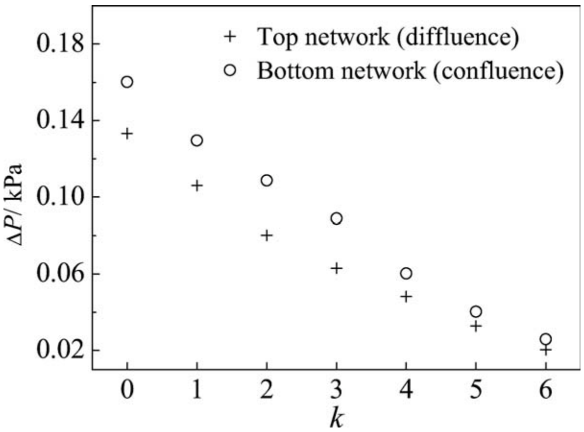

Figure 7. Pressure drop across each branching level ($Re_{k=0}$ = 1500).

confirms the enhancement of heat transfer in the reduction of the channel scale. Influenced by the constructal tree-shaped networks, especially the 0th branching level inlet channel, the temperatures of fluid flowing into each of the highest branching level channels of the bottom network are not identical. Lower inlet fluid temperature will perform in the bottom highest branching level channels which are near the 0th branching level inlet channel of the top networks. Figure 8e shows the temperature distributions of the *x-y* sections at *h*/2 in the serpentine flow pattern heat sink, the temperature uniformity is obviously worse than that in the constructal tree-shaped minichannel networks.

Evaluation of heat transfer performance

Temperature uniformity of the heating surface and the coefficient of performance (COP) are two main factors to evaluate the cooling system performance. In this paper, the

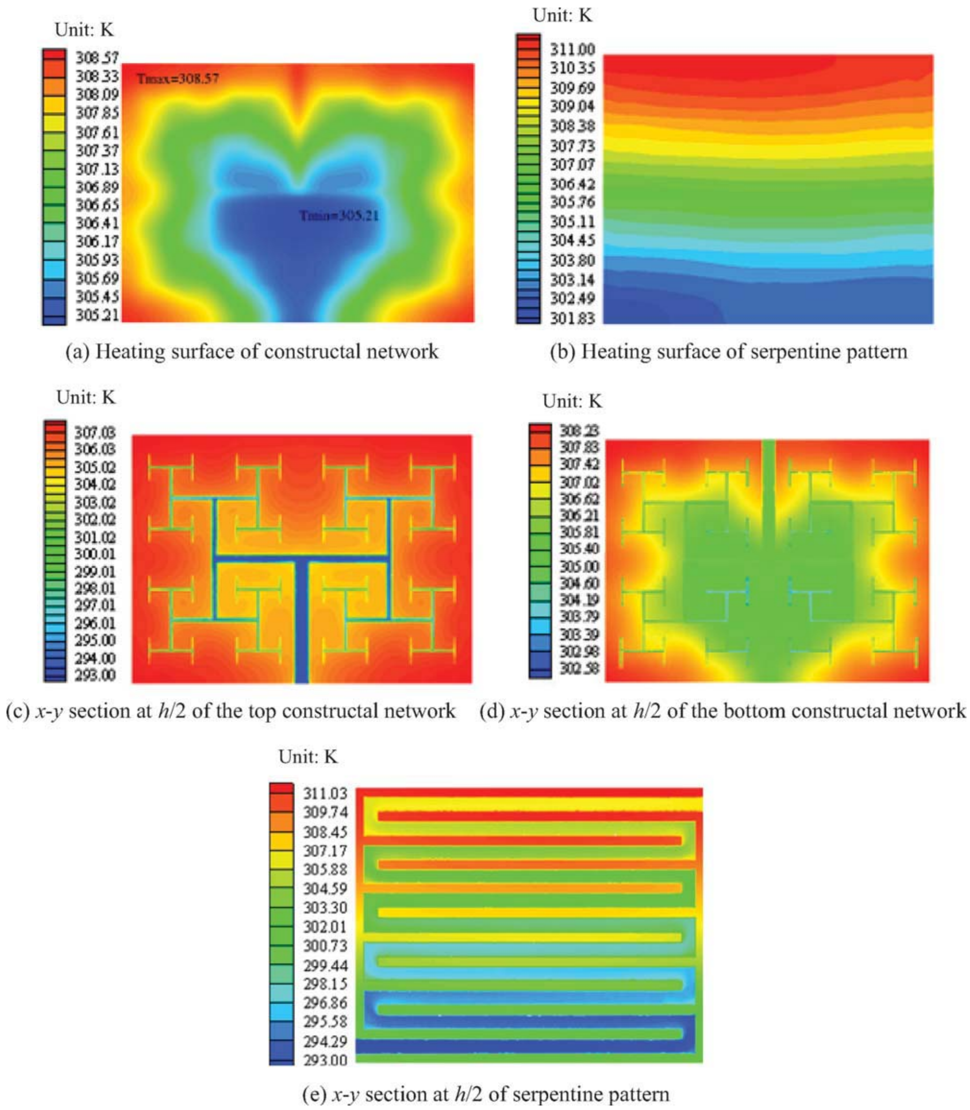

Figure 8. Temperature distributions at different sections (constant heat flux boundary condition: q = 2.5 W/cm^2; $Re_{k=0}$ = 1500).

[Color figure can be viewed in the online issue, which is available at www.interscience.wiley.com.]

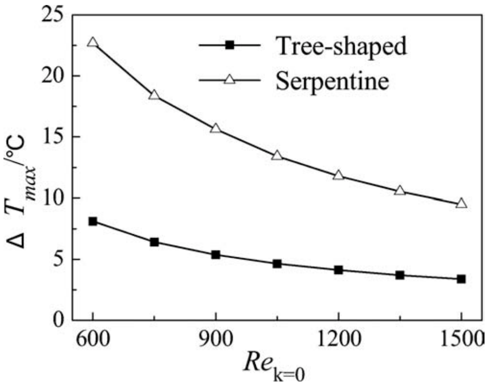

Figure 9. Maximum temperature difference vs. inlet Reynolds number (constant heat flux boundary condition: q = 2.5 W/cm^2).

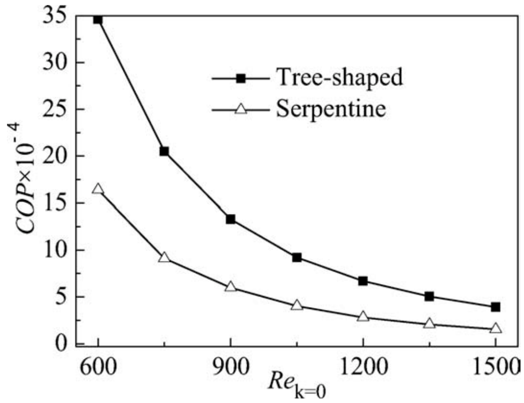

Figure 10. Coefficient of performance vs. inlet Reynolds number (constant temperature boundary condition: T_b = 60°C).

temperature uniformity is evaluated by the maximum temperature difference $\Delta T_{\max}$ on the heating surface under the constant heat flux. The maximum temperature difference $\Delta T_{\max}$ is defined as

$$\Delta T_{\max} = T_{b,\max} - T_{b,\min} \tag{18}$$

where $T_{b,\max}$ and $T_{b,\min}$ are the maximum and minimum temperature on the heating surface respectively.

Another evaluation factor, coefficient of performance (COP) is defined as the ratio of the total heat transfer rate to the pumping power of the fluid flow under the constant temperature condition.

$$\mathrm{COP} = \frac{Q}{q_v \Delta P} \tag{19}$$

Figure 9 shows the maximum temperature difference on the heating surface vs. inlet Reynolds number of both the constructal tree-shaped minichannel heat sink and the serpentine flow pattern heat sink. As shown in the figure, the maximum temperature difference decreases with increasing inlet Reynolds number in both two heat sinks. The maximum temperature difference in the constructal tree-shaped minichannel heat sink is much smaller than that in the serpentine flow pattern heat sink, which proves once again the superiority of temperature uniformity in the constructal tree-shaped minichannel heat sink.

Figure 10 shows the coefficient of performance vs. inlet Reynolds number for both constructal tree-shaped minichannel heat sink and the serpentine flow pattern heat sink. The coefficient of performance of the constructal tree-shaped minichannel heat sink is more than twice as much as that of traditional serpentine flow pattern heat sink. It indicates that more heat current is convected by a tree-shaped channel for the same pumping power. In other words, the constructal tree-shaped minichannel heat sink is proved to provide superior heat transfer performance.

Therefore, the inherent advantages of heat transfer performance including the temperature uniformity and coefficient of performance make constructal tree-shaped heat sinks promising in electronic cooling and chemical process application.

Experimental Verification

Experimental apparatus. To verify the accuracy of the model developed in this paper, an aluminum constructal

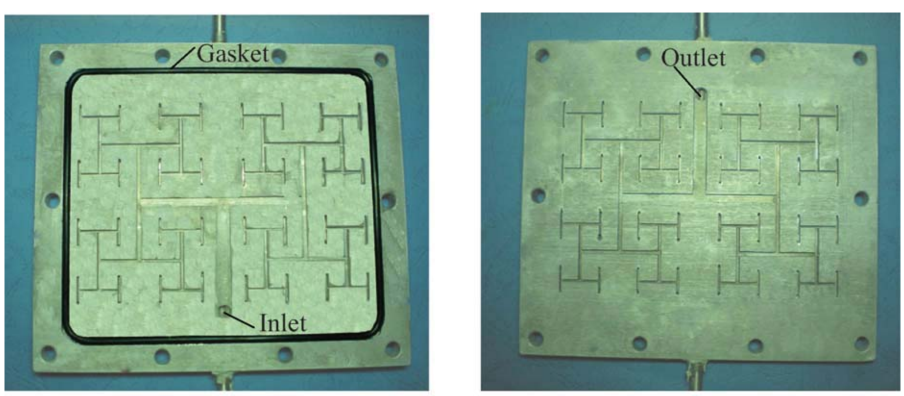

(a) (b)

Figure 11. Image of the mid-plate for aluminum constructal tree-shaped minichannel heat sink: (a) top surface and (b) bottom surface.

[Color figure can be viewed in the online issue, which is available at www.interscience.wiley.com.]

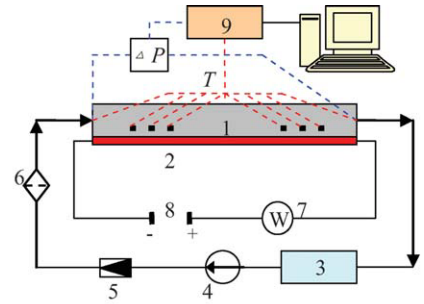

1. Constructal tree-shaped minichannel heat sink 2. Electrical heating plate

3. Constant temperature water-bath 4. Pump 5. Flowmeter 6. Filter

7. Wattmeter 8. DC supply 9. Data acquisition

Figure 12. Schematic of experimental setup.

[Color figure can be viewed in the online issue, which is available at www.interscience.wiley.com.]

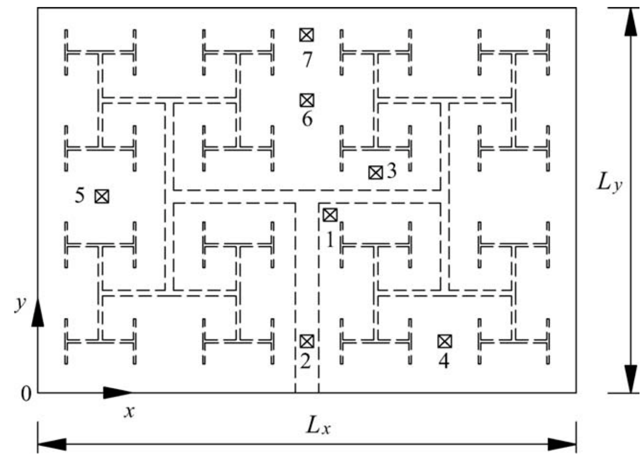

Figure 13. Temperature measuring points on the heating surface.

tree-shaped minichannel heat sink (see Figure 11) with the same geometry dimensions in the simulation is fabricated. An experiment is conducted to measure the temperature distribution on the heating surface and the pressure drop between the inlet and outlet of this aluminum heat sink. Figure 12 shows the schematic of the experimental setup.

Gasket sealing is used in the connection of the top, middle and bottom plate. Bolts connect the electrical heater with the heat sink. Thermally conductive grease is painted on the heating surface to reduce the thermal contact resistance. The whole test section is covered with the thermal insulation materials to limit the heat loss.

The constant heat flux is supplied by the electrical heater, and the power is measured by the wattmeter. The cooling fluid is the deionized water which is maintained at the constant temperature of 20°C by the constant temperature water-bath. The volume flow rate of water flowing through the heat sink is measured by a glass rotor flow meter (accuracy: ±0.4 L/h). The pressure difference between the inlet and outlet of the heat sink is measured by the differential pressure transducer (CYR-302, accuracy: ±0.5%). According to the numerical results, seven temperature measuring points, which are numbered from the lower to the higher temperature, are deposited on the heating surface, as shown in Figure 13. K-type thermocouples (accuracy: ±0.1°C) are utilized to measure both the fluid and heating surface temperatures. The temperature and pressure data is collected by Agilent 34970A data acquisition.

When considering the inlet and outlet pressure loss, the pressure drop is amended as

$$\Delta p = \Delta p_{\text{total}} - \Delta p_{\text{in}} - \Delta p_{\text{out}} \tag{20}$$

where Δp_{total} is the measured pressure drop by the differential pressure transducer, Δp_{in} is the pressure loss between the pressure transducer and inlet, Δp_{out} is the pressure loss between the pressure transducer and outlet. The values of Δp_{in} and Δp_{out} are determined by[41]

$$\Delta p_{\text{in}} = f\frac{l_{\text{in}}}{d_0}\frac{\rho\bar{u}^2}{2} + \zeta_{\text{in}}\frac{\rho\bar{u}^2}{2} \tag{21}$$

$$\Delta p_{\text{out}} = f\frac{l_{\text{out}}}{d_0}\frac{\rho\bar{u}^2}{2} + \zeta_{\text{out}}\frac{\rho\bar{u}^2}{2} \tag{22}$$

Experimental results. Table 2 compares the experimental temperature data and the simulation results with the inlet Reynolds number of 600 and 1500 respectively. Figure 14 presents the maximum and minimum temperatures on the heating surface from both the experiment and simulation for different inlet coolant Reynolds numbers. The comparisons in Table 2 and Figure 14 verify the positive agreement of the experimental temperature data with the simulation results. Figure 15 compares the experimental pressure drop and the simulation results; an agreement is found there as well. Therefore, the accuracy and reliability of the three-dimensional flow and heat transfer model developed in this paper can be verified. And the experiment also examines the fact that the constructal tree-shaped minichannel heat sink

Table 2. Comparison of Experimental Data with Simulation Results

No.	Coordinate (x, y)/mm	$Re_{k=0} = 600$			$Re_{k=0} = 1500$		
		$T_{b,s}$/°C Simulation	$T_{b,e}$/°C Experiment	$T_{b,s} - T_{b,e}$/°C	$T_{b,s}$/°C Simulation	$T_{b,e}$/°C Experiment	$T_{b,s} - T_{b,e}$/°C
1	(75, 46.2)	47.2	45.5	1.7	32.3	31.0	1.3
2	(69, 13.5)	47.3	46.2	1.1	33.4	31.6	1.8
3	(87, 57)	49.5	48.8	0.7	34.3	33.6	0.7
4	(104.6, 13.5)	51.7	50.9	0.8	35.2	34.6	0.6
5	(16.5, 51)	52.9	50.9	2.0	35.5	34.7	0.8
6	(69, 76)	53.0	51.6	1.4	35.7	35.5	0.2
7	(69, 93)	53.8	51.8	2.0	35.9	35.6	0.3

has considerable advantages of superior temperature uniformity and lower pumping power requests.

Here we must mention that, the viscosity of the working fluid (water) decreases with increasing temperature. To transport a fixed mass flow rate, a lower pressure drop occurs due to the decreased viscosity, however, the Reynolds number, by definition, increases with decreasing viscosity, which tends to contribute to increase of pressure drop.[21] In addition, the surface roughness of the channel[42,43] due to machining also may result in an increase of pressure drop. Therefore, the temperature dependence of viscosity and rough surface due to machining may be the dominant reason why the constant deviation of pressure drops occurs.

Conclusions

A three-dimensional model for heat transfer and fluid flow in a constructal tree-shaped minichannel heat sink is developed in this paper. The laminar convective heat transfer in both the constructal tree-shaped minichannel heat sink and the traditional serpentine flow pattern heat sink is numerically analyzed with the consideration of the conjugate heat transfer in channel walls. Furthermore, a constructal tree-shaped minichannel heat sink is designed and fabricated to conduct the verification experiment for the numerical simulation. The conclusions can be summarized as follows:

(1) The strong and weak heat flow can be effectively allocated in tree-shaped flow structures, so the inherent advantage of temperature uniformity of the heating surface in the constructal tree-shaped heat sink is demonstrated.

(2) In tree-shaped networks, the local pressure loss due to confluence flow is larger than that due to diffluence flow.

(3) The constructal tree-shaped minichannel heat sink has the considerable advantage over the traditional serpentine flow pattern in both temperature uniformity and pressure drop. The maximum temperature difference of the constructal tree-shaped minichannel heat sink is far less than that of the traditional serpentine flow pattern heat sink at the same inlet Reynolds number. And the constructal tree-shaped minichannel heat sink also provides a higher coefficient of performance and heat transfer capability.

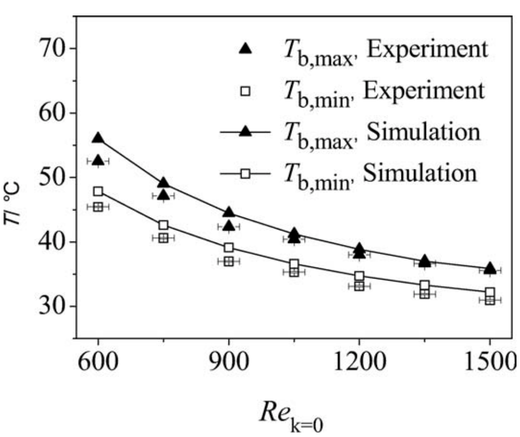

Figure 14. Comparison between experiment and simulation on temperature (constant heat flux boundary condition: q = 2.5 W/cm^2).

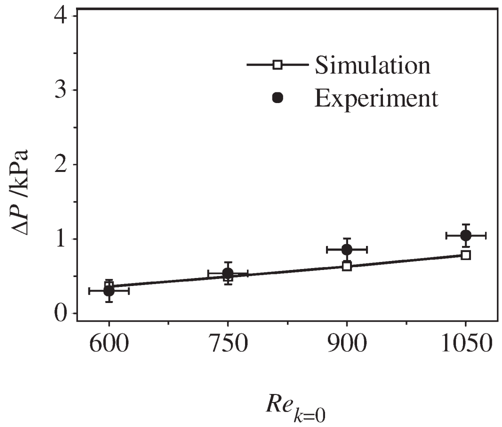

Figure 15. Comparison between experiment and simulation on pressure drop.

(4) The positive agreement of experimental data and simulation results in both pressure drop and temperature distribution verifies that the three-dimensional flow and heat transfer model developed in this paper is reasonable. In addition, the experiment also examines the advantages of superior temperature uniformity and lower pumping power requests.

Acknowledgments

The authors gratefully acknowledge the supports provided by Natural Science Foundation of Jiangsu Province No. BK2008309, Aeronautical Science Foundation No. 2008ZH69001and Research Fund for the Doctoral Program of Higher Education No.20070286072.

Notation

C_p = specific heat capacity (J/kg/K)
D = dimension of channel length distribution
d_k = branch diameter of the kth level (m)
h = depth of channel (m)
f = friction factor
L_k = branch length of the kth level (m)
L_x, L_y, L_z = length of the heat sink in the x, y, z direction (m)
l_{in} = length between the pressure transducer and inlet (m)
l_{out} = length between the pressure transducer and outlet (m)
n = normal direction
$\triangle P$ = pressure drop (Pa)
q = heat flux (W/m^2)
q_v = volume flux (m^3/s)
Q = total heat transfer rate (W)
Re = Reynolds number
T = temperature (K)
$\bar{u}$ = average velocity (m/s)
u, v, w = velocity component in the x, y, z direction respectively, m/s
w_k = branch width of the kth level (m)
x, y, z = Cartesian coordinates (m)

Greek letters

$\triangle$ = diameter dimension
λ = thermal conductivity (W/m/K)
ρ = density (kg/m^3)
μ = dynamic viscosity (kg/m/s)
ζ_{in}, ζ_{out} = loss coefficients for abrupt changes in flow cross section for inlet and outlet
COP = coefficient of performance

Subscripts

k = branching level
b = bottom wall
f = fluid
s = solid
Γ = interface between the solid and fluid
in = inlet
out = outlet
v = volume
max, min = maximum and minimum

Literature Cited

1. Tuckerman DB, Pease RFW. High-performance heat sinking for VLSI. *IEEE Electron Device Lett*. 1981;EDL-2:126–129.
2. Chen YP, Zhang CB, Shi MH, Wu JF. Three-dimensional numerical simulation of heat and fluid flow in noncircular microchannel heat sinks. *Int Commun Heat Mass Transfer*. 2009;36:917–920.
3. Bejan A, Lorente S. *Design with Constructal Theory*. Hoboken, NJ: Wiley, 2008.
4. Bejan A. *Shape and Structure, from Engineering to Nature*. Cambridge: Cambridge University Press, 2000.
5. Mandelbrot BB. *The Fractal Geometry of Nature*. New York, NY: W. H. Freeman, 1982.
6. Bejan A. Constructal-theory network of conducting paths for cooling a heat generating volume. *Int J Heat Mass Transfer*. 1997;40:799–816.
7. Senn SM, Poulikakos D. Laminar mixing, heat transfer and pressure drop in tree-like microchannel nets and their application for thermal management in polymer electrolyte fuel cells. *J Power Sources*. 2004;130:178–191.
8. Senn SM, Poulikakos D. Tree network channels as fluid distributors constructing double-staircase polymer electrolyte fuel cells. *J Appl Phys*. 2004;96:842–852.
9. Senn SM, Poulikakos D. Pyramidal direct methanol fuel cells. *Int J Heat Mass Transfer*. 2006;49:1516–1528.
10. Vargas JVC, Bejan A. Thermodynamic optimization of internal structure in a fuel cell. *Int J Energy Res*. 2004;28:319–339.
11. Vargas JVC, Ordonez JC, Bejan A. Constructal flow structure for a PEM fuel cell. *Int J Heat Mass Transfer*. 2004;47:4177–4193.
12. Bejan A. Street network theory of organization in nature. *J Adv Transport*. 1996;30:85–107.
13. Bejan A, Errera MR. Deterministic tree networks for fluid flow: geometry for minimal flow resistance between a volume and one point. *Fractals*. 1997;5:685–695.
14. Bejan A. The tree of convective heat streams: its thermal insulation function and the predicted 3/4-power relation between body heat loss and body size. *Int J Heat Mass Transfer*. 2001;44:699–704.
15. Bejan A, Lorente S. The constructal law and the thermodynamics of flow systems with configuration. *Int J Heat Mass Transfer*. 2004;47:3203–3214.
16. Bejan A, Lorente S. Constructal theory of generation of configuration in nature and engineering. *J Appl Phys*. 2006;100:041301, 1–27.
17. Kearney MM. Engineering fractals enhance process applications. *Chem Eng Prog*. 2000;96:61–68.
18. Luo LG, Fan ZW, Gall HL, Zhou XG, Yuan WK. Experimental study of constructal distributor for flow equidistribution in a mini crossflow heat exchanger (MCHE). *Chem Eng Process*. 2008;47: 229–236.
19. Pence DV. Improved thermal efficiency and temperature uniformity using fractal-like branching channel networks. Proceedings of the International Conference on Heat Transfer and Transport Phenomena in Micro Scale. Banff, Canada, Begell House, 2000:142–148.
20. Pence DV. Reduced pumping power and wall temperature in microchannel heat sinks with fractal-like branching channel networks. *Microscale Thermophys Eng*. 2002;6:319–330.
21. Alharbi AY, Pence DV, Cullion NR. Fluid flow through microscale fractal-like branching channel networks. *J Fluids Eng*. 2003;6: 1051–1057.
22. Alharbi AY, Pence DV, Cullion NR. Thermal characteristics of microscale fractal-like branching channels. *J Heat Transfer*. 2004; 126:744–752.
23. Daniels B, Liburdy JA, Pence DV. Adiabatic flow boiling in fractal-like microchannels. *Heat Transfer Eng*. 2007;28:817–825.
24. Daniels BJ, Liburdy JA, Pence DV. Experimental studies of adiabatic flow boiling in fractal-like branching microchannel. *IMECE 2008: Heat Transfer Fluid Flow Therm Syst*. 2009;10:107–117.
25. Wechsatol W, Lorente S, Bejan A. Optimal tree-shaped networks for fluid flow in a disc-shaped body. *Int J Heat Mass Transfer*. 2002; 45:4911–4924.
26. Ghodoossi L. Optimization of tree-shaped fluid networks with size limitations. *Int J Therm Sci*. 2007;46:434–443.
27. Ghodoossi L. Thermal and hydrodynamic analysis of a fractal microchannel network. *Energy Conversion Manage*. 2005;46:771–788.
28. Chen YP, Cheng P. Heat transfer and pressure drop in fractal tree-like microchannel nets. *Int J Heat Mass Transfer*. 2002;45:2643–2648.
29. Xu P, Yu BM. The scaling laws of transport properties for fractal-like tree networks. *J Appl Phys*. 2006;100:104906, 1–8.
30. Wang XQ, Mujumdar AS, Christopher Y. Numerical analysis of blockage and optimization of heat transfer performance of fractal-like microchannel nets. *J Electron Packaging*. 2006;128:38–45.
31. Wang XQ, Mujumdar AS, Christopher Y. Thermal characteristics of tree-shaped microchannel nets for cooling of a rectangular heat sink. *Int J Therm Sci*. 2006;45:1103–1112.
32. Hong FJ, Cheng P, Ge H, Teck Joo G. Conjugate heat transfer in fractal-shaped microchannel network heat sink for integrated microelectronic cooling application. *Int J Heat Mass Transfer*. 2007;50: 4986–4998.
33. Hong FJ, Cheng P, Ge H, Teck Joo G. Design of a fractal tree-like microchannel net heat sink for microelectronic cooling. Proceedings of 4th International Conference on Nanochannels Microchannels and Minichannels (ICNMM). Limerick, Ireland, American Society of Mechanical Engineers, 2006:305–312.
34. Wechsatol W, Lorente S, Bejan A. Tree-shaped flow structures with local junction losses. *Int J Heat Mass Transfer*. 2006;49:2957–2964.
35. Wang XQ, Mujumdar AS, Christopher Y. Effect of bifurcation angle in tree-shaped microchannel networks. *J Appl Phys*. 2007;102: 073530, 1–8.
36. Wechsatol W, Lorente S, Bejan A. Tree-shaped insulated designs for the uniform distribution of hot water over an area. *Int J Heat Mass Transfer*. 2001;44:3111–3123.
37. Wechsatol W, Lorente S, Bejan A. Development of tree-shaped flows by adding new users to existing networks of hot water pipes. *Int J Heat Mass Transfer*. 2002;45:723–733.
38. Escher W, Michel B, Poulikakos D. Efficiency of optimized bifurcating tree-like and parallel microchannel networks in the cooling of electronics. *Int J Heat Mass Transfer*. 2009;52:1421–1430.
39. Bejan A, Rocha LAO. Lorente S. Thermodynamic optimization of geometry: T-and Y-shaped constructs of fluid streams. *Int J Therm Sci*. 2000;39:949–960.
40. Murray CD. The physiological principle of minimum work. I. The vascular system and the cost of blood volume. *Proc Natl Acad Sci USA*. 1926;12:207–214.
41. Shames IH. *Mechanics of Fluids*. New York, NY: McGraw-Hill, 1992.
42. Chen YP, Zhang CB, Shi MH, Peterson GP. Role of surface roughness characterized by fractal geometry on laminar flow in microchannels. *Phys Rev E* 2009;80:026301, 1–7.
43. Kandlikar SG. Exploring roughness effect on laminar internal flow-are we ready for change. *Nanoscale Microscale Thermophys Engineering* 2008;12:61–82.

Manuscript received Jun. 8, 2009, revision received Sept. 22, 2009, and final revision received Nov. 12, 2009.